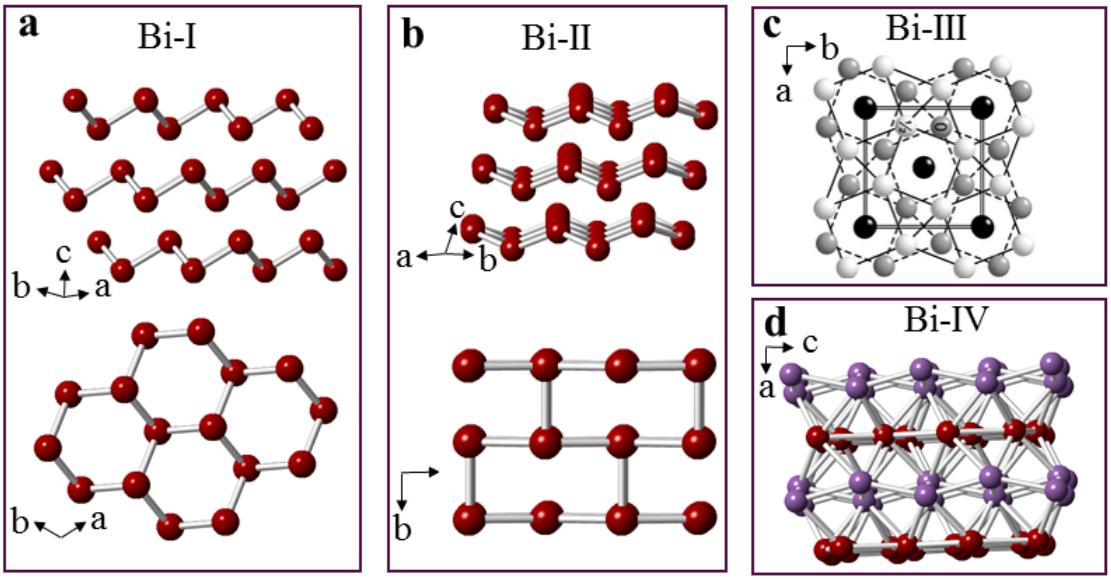


**Supplementary Figure 1 | Crystal structures of different Bi phases.** (**a**) Structure of Bi-I[1]. (**b**) Structure of Bi-II[2]. (**c**) Structure of Bi-III[3]. (**d**) Structure of Bi-IV[4].

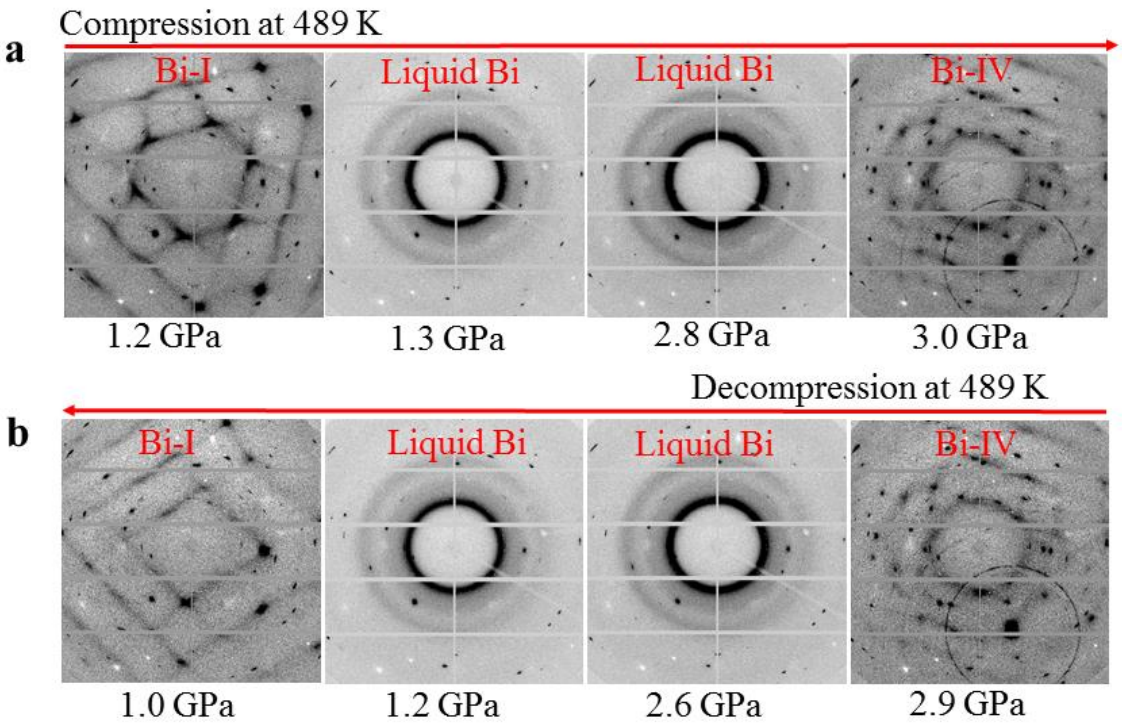


**Supplementary Figure 2 | Diffraction images at 489 K with NaCl as pressure medium.** (**a**) Sample Bi was compressed from 0.5 GPa to 3.2 GPa (Right red arrow). Bi-I phase transforms to liquid Bi at ~1.3 GPa, followed by crystallization into Bi-IV at ~2.8 GPa. (**b**) Sample Bi is decompressed from 3.2 GPa to 0.5 GPa (left red arrow). Bi-IV melts into liquid Bi at ~2.6 GPa, followed by crystallization into Bi-I at ~1.2 GPa. The background is subtracted for all images. The diffraction spots in liquid Bi come from the pressure medium of NaCl or the diamond anvils.

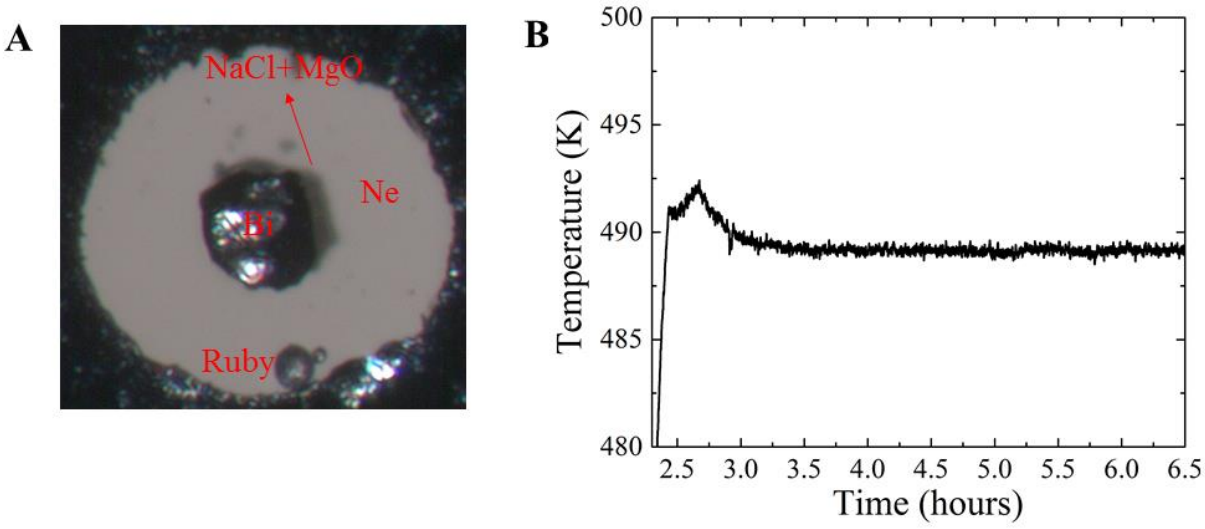


**Supplementary Figure 3 | Photo of a sample chamber after gas loading and typical temperature variations in experiments.** (**a**) A photo of a sample chamber at 0.5 GPa after neon was loaded. The sample chamber is ~150 μm in diameter, and the bismuth sample dimension is 30×30 μm. (**b**) Typical temperature variations recorded as a function of time during one experiment. The Bi sample is compressed and decompressed after temperature becomes stable within a degree.

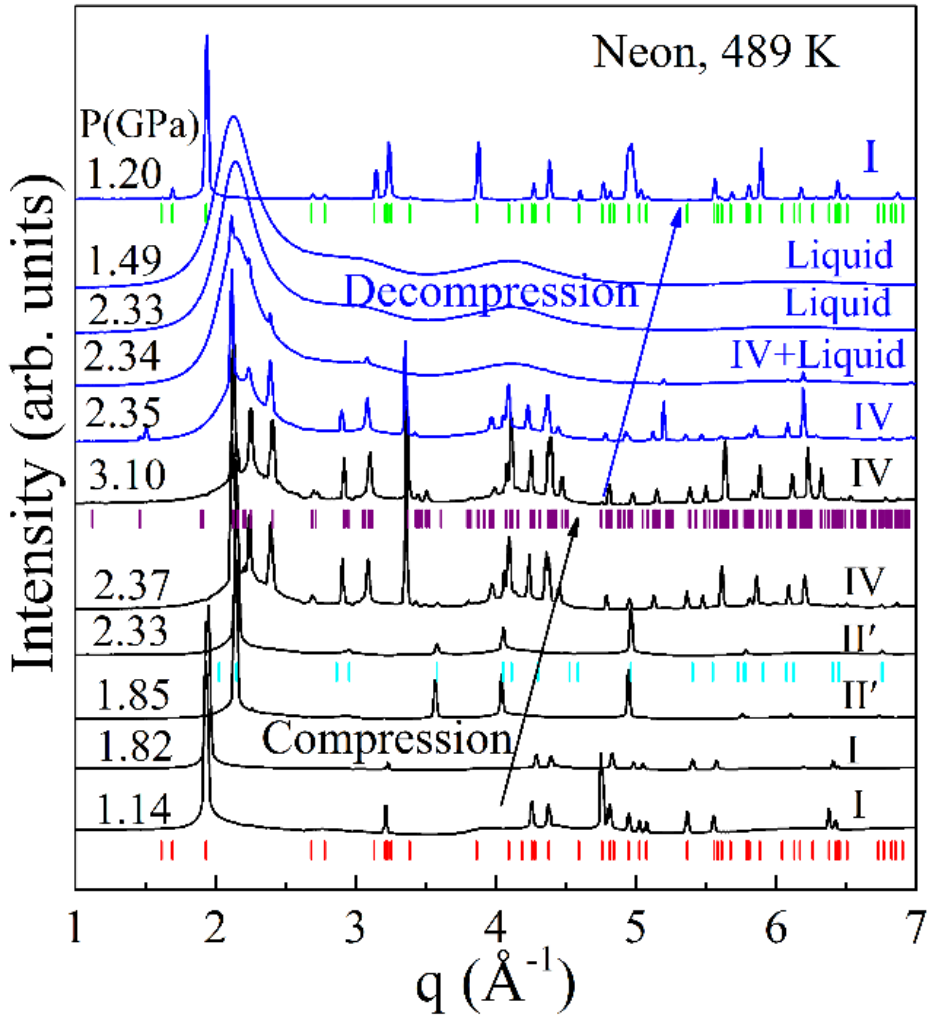


**Supplementary Figure 4 | Integrated x-ray diffraction patterns of Bi at 489 K.** The Bi sample is compressed and decompressed at hydrostatic condition with neon as pressure medium. Upon compression (black arrow). Bi-I phase transforms to Bi-II´ at ~1.8 GPa, followed by II´-to-IV transition at ~2.4 GPa. Blue arrow indicates that Bi is decompressed from 3.1 GPa to 1.0 GPa. Bi-IV melts into liquid Bi at ~2.3 GPa, followed by crystallization of liquid Bi at ~1.2 GPa. The symbol bars below each of the corresponding diffraction patterns indicate the indexing of the crystal phases.

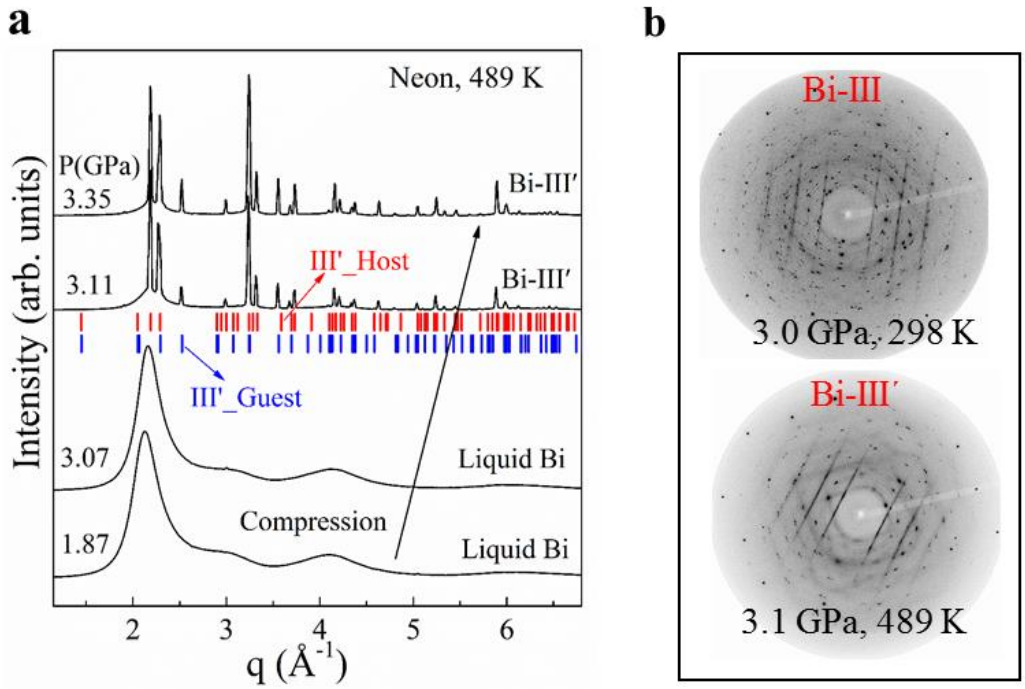


**Supplementary Figure 5 | Phase transition of DIL under hydrostatic condition at 489 K.** Neon is used as pressure medium. (**a**) The DIL is compressed from ~1.9 GPa to 3.3 GPa. It crystallizes into Bi-III-like phase (Bi-III´) at ~3.1GPa, which can be indexed using a mixture of two body-centered-tetragonal phases (red and blue bars). The lattice parameters are close to those of the host and guest structures of Bi-III at ~3 GPa[1]. (**b**) Comparison of diffraction images of Bi-III´ and Bi-III. There are similar straight diffuse scattering lines in both Bi-III and Bi-III´, which comes from the disordered guest chains[5-9].

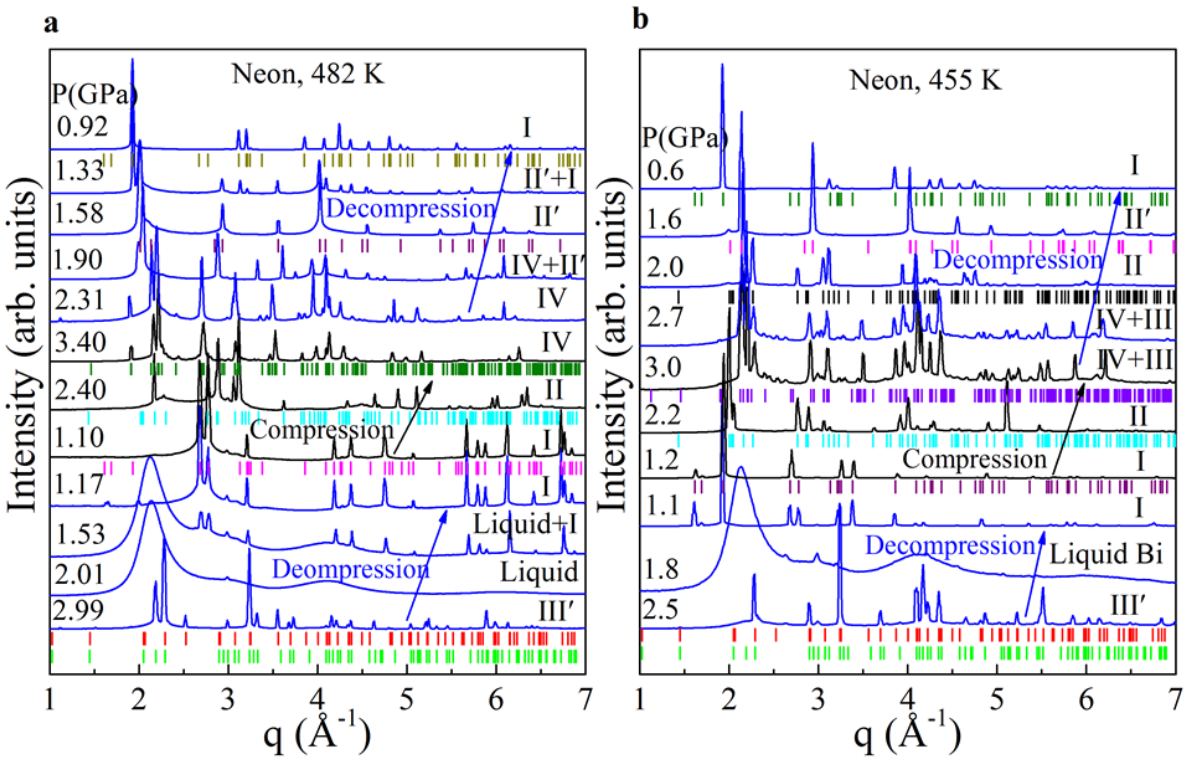


**Supplementary Figure 6 | Integrated x-ray diffraction patterns of Bi under hydrostatic condition.** Neon is used as pressure transmitting medium. (**a**) Sample is decompressed from ~3.0 GPa to 1.1 GPa (blue arrow) at 482 K. III´→ liquid→ I transitions are observed. Then sample is compressed from 1.1 GPa to 3.4 GPa with I→ II→ IV transitions (black arrow). When the starting phase is IV, IV→ II´→ I transitions appear (blue arrows on the top). (**b**) Sample is decompressed and compressed at 455 K. When decompressing Bi-III´, III´→ liquid→ I transitions are observed while decompressing mixture of IV+III led to IV+III→ II→ I transitions. Under compression, I→ II→ IV transitions appear. The symbol bars below the corresponding diffraction patterns indicate the indexing of the crystal phases.

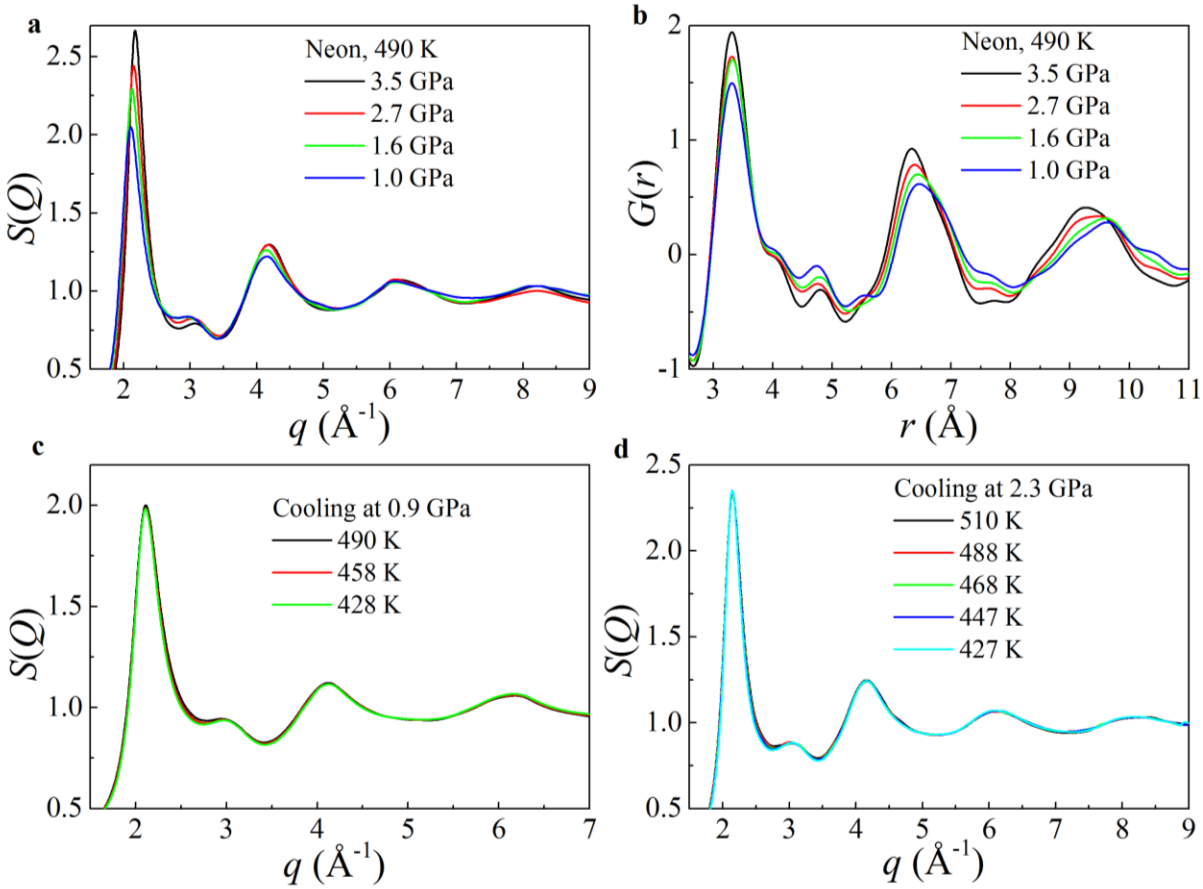


**Supplementary Figure 7 | Effect of temperature and pressure on the structure of DIL and supercooled liquid.** (**a**) Evolution of structure factors, S(*Q*), of the DIL under various pressures at 490 K. (**b**) Reduced pair distribution functions, *G*(*r*) of the DIL under pressures. (**c**) *S*(*Q*) of the supercooled liquid Bi at 0.9 GPa. (**d**) *S*(*Q*) of the supercooled liquid Bi at 2.3 GPa.

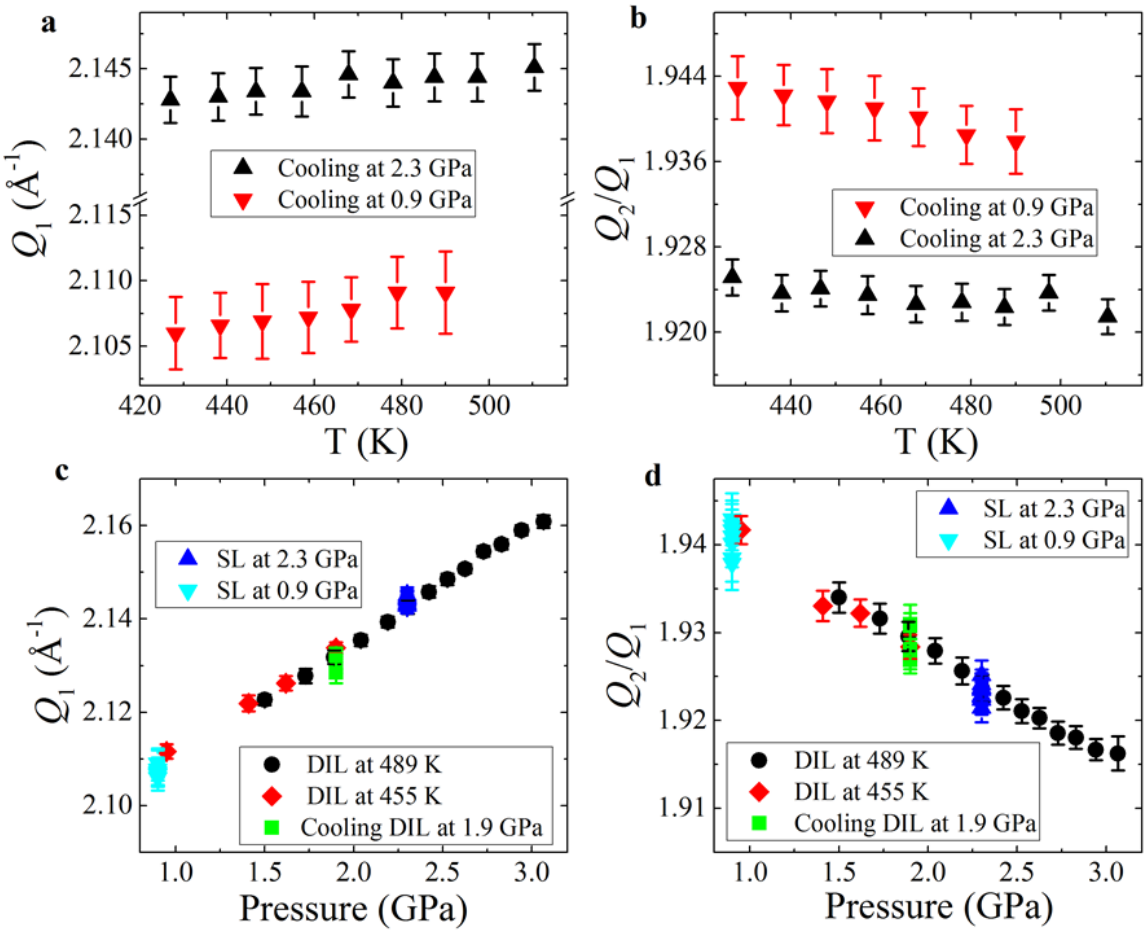


**Supplementary Figure 8 | Pressure and temperature dependences of $Q_1$ and $Q_2/Q_1$ of the DIL and the supercooled liquid.** (**a**) and (**b**) Temperature-dependence of $Q_1$ and $Q_2/Q_1$ under cooling at 0.9 GPa and 2.3 GPa, respectively. $Q_1$ decreases slightly during cooling while $Q_2/Q_1$ increases slightly with cooling. (**c**) and (**d**) Pressure-dependences of $Q_1$ and $Q_2/Q_1$ of the DIL. When the data of supercooled liquid Bi in (**a**) and (**b**) were over-plotted on (**c**) and (**d**), we find that $Q_1$ and $Q_2$ of the supercooled liquid at different temperatures are close to those of the DIL at corresponding pressures, indicating the structural similarity of the DIL with the supercooled liquid.

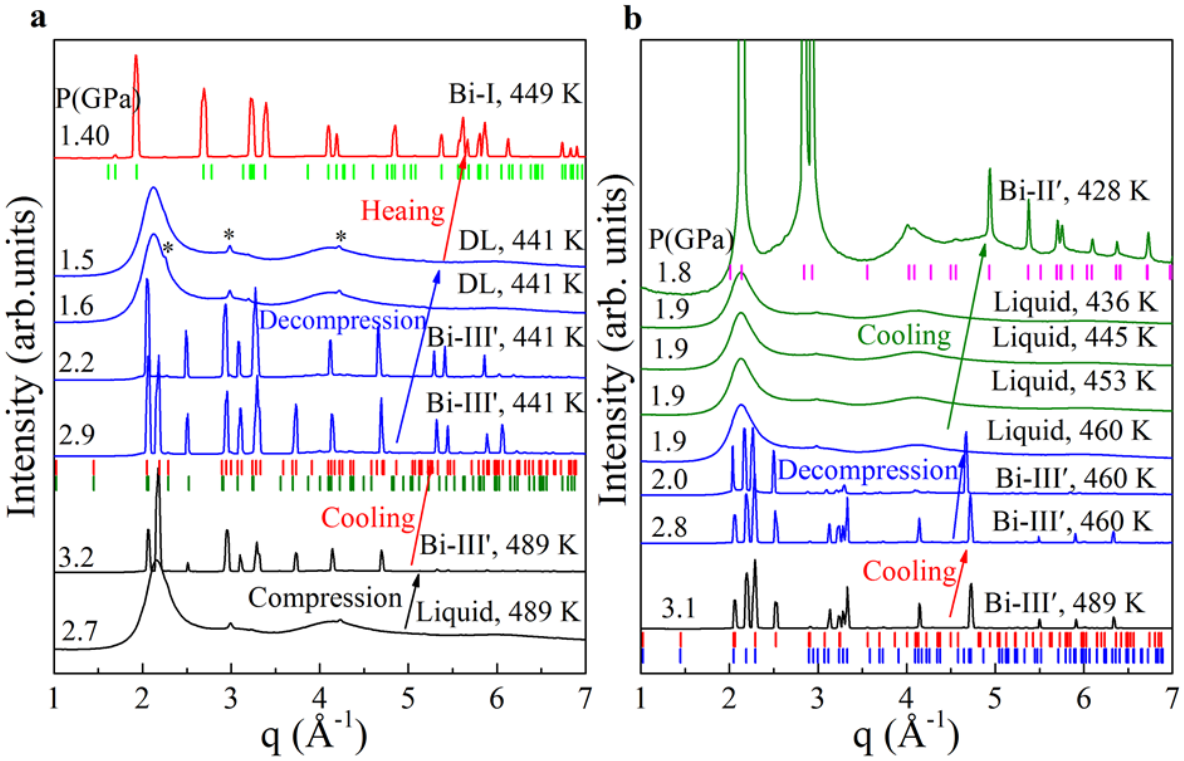


**Supplementary Figure 9 | Crystallization of the DIL under heating and cooling.** Bi-III´ is obtained by compressing liquid Bi above 489 K. (**a**) The DIL is compressed at 489 K and transformed to Bi-III´. Then Bi-III´ is cooled from 489 K to 441 K. Keeping the temperature at 441 K, Bi-III´ is decompressed and melts into a liquid state under decompression. After DIL is obtained at 441 K, the metastable liquid Bi is heated from 441 K to 449 K and crystallizes into Bi-I during heating. After crystallization, the pressure changes from 1.5 GPa to 1.4 GPa. (**b**) Decompression-induced liquid crystallizes into Bi-II under cooling from 460 K to 428 K. The pressure changes from 1.9 GPa to 1.8 GPa after crystallization.

**Supplementary Table 1 | Unit cell parameters of Bi-IV, III´, II, II´ and I. The structural models of these crystalline phases are from Refs. 1, 2, 4, 10.**

| | IV (2.97 GPa) | III´ (3.46 GPa) | | II (2.0 GPa) | II´ (2.0 GPa) | I (1.14 GPa) |
|---|---|---|---|---|---|---|
| Structure | Orthorhombic (*Cmca*) | Tetragonal (host: *I4/mcm*) | Tetragonal (Guest: *I4/mmm*) | Monoclinic (*C2/m*) | Tetragonal | Hexagonal |
| *a* | 11.178(1) Å | 8.673(3) Å | 8.670(3) Å | 6.663(4) Å | 6.222(3) Å | 4.522(1) Å |
| *b* | 6.618(1) Å | | | 6.181(3) Å | | |
| *c* | 6.596(1) Å | 4.266(5) Å | 3.247(3) Å | 3.312(1) Å | 3.320(1) Å | 11.681(3) Å |
| *β* | | | | 110.93(2)° | | |
| *V* | 487.92 (9) $Å^3$ | 320.9(3) Å3 | 244.1(2) $Å^3$ | 127.39(5) $Å^3$ | 128.5(1) $Å^3$ | 206.90(5) $Å^3$ |

**Supplementary Table 2 Summary of the phase transitions under hydrostatic condition and different temperatures.** Red text indicates the occurrence of decompression-induced liquid, i.e., crystal-liquid-crystal transitions, while crystal-crystal-crystal transitions are observed under compression. The last column indicates the numbers of repeated experiments at corresponding temperatures. In each experimental run, a fresh sample is used.

| T (K) | Compression | Decompression | Times |
|---|---|---|---|
| 505 | I → Liquid → Bi-N | IV → Liquid → I | 1 |
| 489 | I → II′→ IV | IV→ Liquid→ I | 5 |
| | Liquid→ III′ | III′ → Liquid → I | 5 |
| 482 | | III′ → Liquid→ I | 1 |
| | I→ II→ IV | IV → II′ → I | 1 |
| 455 | | III′ → Liquid → I | 2 |
| | I→ II→ IV+III | IV+III → II→ II′ →I | 2 |
| 441 | I→ II→ III | III′ → Liquid → I | 1 |
| 423 | I→ II→ III | III′ → II → I | 2 |

## SUPPLEMENTARY REFERENCES:


1. Katzke, H. & Toledano, P. Displacive mechanisms and order-parameter symmetries for the A7-incommensurate-bcc sequences of high-pressure reconstructive phase transitions in Group Va elements. *Phys. Rev. B* **77**, 024109 (2008).
2. Akselrud, L. G., Hanfland, M. & Schwarz, U. Refinement of the crystal structure of Bi-II, at 2.54 GPa. *Z Krist-New Cryst. St.* **218**, 415-416 (2003).
3. McMahon, M. I., Degtyareva, O. & Nelmes, R. J. Ba-IV-type incommensurate crystal structure in group-V metals. *Phys. Rev. Lett.* **85**, 4896-4899 (2000).
4. Chaimayo, W. *et al.* High-pressure, high-temperature single-crystal study of Bi-IV. *High Pressure Res.* **32**, 442-449 (2012).
5. Nelmes, R. J., Allan, D. R., McMahon, M. I. & Belmonte, S. A. Self-hosting incommensurate structure of barium IV. *Phys. Rev. Lett.* 83, 4081-4084 (1999).
6. McMahon, M. I. & Nelmes, R. J. Chain "melting" in the composite Rb-IV structure. *Phys. Rev. Lett.* 93, 055501 (2004).
7. Falconi, S. et al. X-ray diffraction study of diffuse scattering in incommensurate rubidium-IV. *Phys. Rev. B* 73, 214102 (2006).
8. McBride, E. E. et al. One-dimensional chain melting in incommensurate potassium. *Phys. Rev. B* 91, 144111 (2015).
9. McMahon, M. I., Bovornratanaraks, T., Allan, D. R., Belmonte, S. A. & Nelmes, R. J. Observation of the incommensurate barium-IV structure in strontium phase V. *Phys. Rev. B* 61, 3135-3138 (2000).
10. Principi, E. *et al.* Metastable phase diagram of Bi probed by single-energy x-ray absorption detection and angular dispersive x-ray diffraction. *Phys. Rev. B* **74**, 064101 (2006).